



# The aging behavior of HDPE pipe bodies and butt-fusion welded joints: effects of thermal oxidative and hydrothermal accelerated aging

Ying-Chun Chen<sup>1</sup> · Jie Yang<sup>1</sup> · Yan-Feng Li<sup>1</sup> · Rui Miao<sup>2</sup> · Qiang Li<sup>2</sup> · Xiao-li Fan<sup>2</sup>

Received: 21 December 2023 / Accepted: 1 April 2024  
© The Author(s), under exclusive licence to Springer Nature B.V. 2024

## Abstract

We investigate the aging behavior of High-Density Polyethylene (HDPE) pipelines, specifically comparing the Pipe Body (PB) and Butt-Fusion Welded Joint (BFWJ) under thermal oxidative and hydrothermal accelerated aging conditions. Our results indicate that the performance disparity between PB and BFWJ diminishes as aging time increases. We also find that the specimen type affects the quantity of polyethylene fibers, with hydrothermal aging significantly affecting the cohesive force among these fibers in both PB and BFWJ. These findings on differential aging processes of PB and BFWJ contribute to a deeper understanding of HDPE pipeline durability and offer practical recommendations for mitigating degradation risks associated with these disparities. This research underscores the importance of considering specific aging behaviors in the maintenance and reliability assessment of HDPE pipeline systems used in energy transport, industrial, and agricultural applications.

**Keywords** High-density polyethylene · Thermal oxidative accelerated aging · Hydrothermal accelerated aging · Butt-fusion welded joint · Temperature · Scanning electron microscope

## 1 Introduction

High-density polyethylene (HDPE) represents revolutionary progress in the field of pipelines, often described as “replacing steel with plastic” (Taheri 2013; Pinter and Lang 2003; Barker et al. 1983). With the steady development and growth of HDPE materials, its market is gradually expanding. Specifically, HDPE pipelines exhibit excellent performance in gas transportation (Ghabeche et al. 2019; Esaklul and Jim 2017; Erdmann et al. 2019). HDPE possesses various advantageous properties (Oluwoye et al. 2015, 2016; Bracco et al. 2018; Badia et al. 2012), including cold-hardiness, chemical stability, toughness, mechanical strength, dielectric properties, and resistance to environmental stress cracking.

---

✉ Y.-C. Chen  
yingchun.c@bjut.edu.cn

<sup>1</sup> Beijing University of Technology, Beijing 100124, China

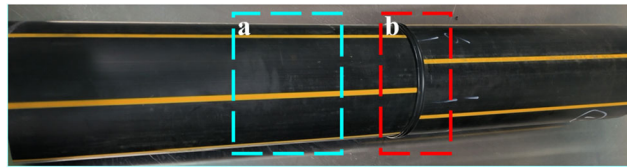
<sup>2</sup> Xinjiang Inspection Institute of Special Equipment, Urumqi, 830011, Xinjiang, China

In actual engineering, the reliability of HDPE pipelines has become a critical concern in scientific research and engineering applications. Long-term oil and gas pipeline reliability is a major safety issue (Chaoui et al. 2008; Choi et al. 2005; Pospíšil et al. 2003; Hoang and Lowe 2008). The natural aging test provides relatively accurate results as its materials are sourced from actual projects (Bhowmick and White 2002; Chen et al. 2019). HDPE butt-fusion welded joints boast high tensile strength, strong corrosion resistance, good sealing performance, and the ability to be quickly and easily installed (Frederick et al. 2010). Therefore, butt fusion welding is extensively used for pipeline connections on HDPE pipeline construction sites (Zheng et al. 2015; Murch and Troughton 1998). The stress-strain and oxidation induction time (OIT) curves of the samples decreased with the increase of aging time at thermal-oxidative aging temperatures of 80, 90, and 100 °C, for aging durations ranging from 0 to 384 hours. However, significant variations were observed in the aging durations selected for the three different thermo-oxidative aging temperatures, as reported by Wang et al. (Wang et al. 2021). Whelton et al. observed significant changes in the properties of polyethylene within 25 days under accelerated aging conditions (Whelton and Dietrich 2009).

The mechanical and chemical properties of polyethylene pipes in long-term service were studied by scholars (Chen et al. 2023; Blivet et al. 2021). The results showed that the crystallinity of polyethylene pipes increased over time. Dominant in the aging reaction were branching-chain and cross-linking reactions of molecular chains. Some scholars also investigated the performance of polymers on a micro-scale under high temperature and pressure conditions of thermal oxidative accelerated aging. Aging degradation of the polymer was found to be primarily affected by aging time (AT), the minimum distance between fiber surfaces, and oxygen pressure.

Some scholars analyzed the crystal orientation of the central axis of unwelded polyethylene pipes. They found differences in elongation between the unwelded polyethylene pipe and the butt joint (Leskovic et al. 2006). Some scholars also investigated the properties of ordinary polyethylene pipes and proposed that the bending fatigue resistance of electric-fusion butt joints and butt-fusion welded joints was lower than that of unwelded pipes (Chen et al. 1997). In 1997, the tensile properties of polyethylene pipe welds were studied to find that the tensile strength and toughness of the welded part were lower than that of the pipe body (Murch and Troughton 1998). Scholars have conducted research on both the pipe and butt-fusion welded joints of the pipe (Lai et al. 2022). They have identified several factors that affect the accuracy of predicting the service life of the pipe during the production process, such as high temperature, oxygen, microstructure, and material properties of the joint, which differ from those of the pipe during the butt-fusion welded joint production (Konica and Sain 2020; Kato and Osawa 1999; S et al. 2004). Remarkably, the impact of oxygen and moisture on the performance of the pipeline are significant factors in the actual pipeline application environment. The life of the butt-fusion welded joint plays a prominent role in predicting pipeline life. Therefore, a comparative experimental study was conducted on the effects of thermal oxidative accelerated aging and hydrothermal accelerated aging methods on the performance of the pipe and butt-fusion welded joint.

In this study, Pipe Body and Butt-Fusion Welded Joint (PB and BFWJ) of PE100 were the research objects, and they underwent accelerated aging tests at 80 °C during thermal-oxidative aging and hydrothermal aging. PB and BFWJ underwent separate performance tests, and the performance differences and the reasons for these differences between them during different accelerated aging methods were compared and analyzed. The differences in aging mechanisms between pipes and joints were studied. The results of this paper help supplement the research on the difference in aging behavior between HDPE pipe and butt-fusion welded joints.

**Fig. 1** PE100 pipe body and butt-fusion welded joint**Table 1** Information on the pipe body and butt-fusion welded joint used in the study

Grade	Minimum Wall Thickness $e_{\min}$ (mm)	Density ( $\text{g}/\text{cm}^3$ )	Nominal Diameter (mm)	Standard Dimension Ratio
PE100	10	0.94	110	11

**Table 2** The details of the accelerated aging scheme

Specimen	Materials	Accelerated Aging Type	Temperature	Accompanying Conditions
1	New pipeline	–	$23 \pm 0.5$ °C	–
2	New butt-fusion welded joint			
3	New pipeline	Thermal oxidative aging	80 °C	Oxygen
4	New butt-fusion welded joint			
5	New pipeline	Hydrothermal aging		Water
6	New butt-fusion welded joint			

## 2 Experimental

### 2.1 Material

In this study, PE100, produced by Yada Plastic Products Co., was selected as the experimental raw material. For this examination, area ‘a’ is selected on the pipe body specimen, while area ‘b’ is designated on the butt-fusion welded joint specimen in Fig. 1. Table 1 provides additional information about the testing of the PE100. Table 2 is the details of the accelerated aging scheme.

### 2.2 Accelerated aging

In this study, we employed thermal oxidative accelerated aging and hydrothermal accelerated aging at the same temperature for accelerated aging. The PB and BFWJ of PE100 were aged for 240 h, 480 h, 720 h, and 960 h in drying and water bath boxes, both set at 80 °C respectively. Specimens were removed in batches according to various aging durations to ensure consistency in the experimental environment. Subsequently, the mechanical and chemical properties of specimens with various aging times were tested.

**Table 3** The scheme for performance testing and chemical characterization

Test Type	Sample Production and Testing		Test Instrument	Test Temperature	Sample Results
	Chinese National Standard	International Standard			
Impact testing	GB/T 1043.1 (2008)	ISO 179-1 (2010)	PTM2200	23 ± 0.5 °C	Average of 5 parallel tests per group
Tensile testing	GB/T 19810 (2005)	ISO 13953 (2001)	ETM204C		
Hardness	GB/T 38119 (2019)	–	LX-D model Shore hardness tester		Take the average of 18 test values per group.
Vicat softening temperature	–	ISO 2507-1 (1995)	HVT302B	–	Average of 3 parallel trials per group
Oxidation induction time (OIT)	GB/T 19,466.6 (2009)	ISO 11357-6 (2013)	DSC-500B	–	

### 2.3 Test methods

Following the aging tests, we conducted impact tests, tensile tests, hardness tests, Vicat softening temperature measurements, OIT assessments, attenuated total Fourier transform reflection infrared spectroscopy, and scanning electron microscope (SEM) tests on the PB and BFWJ. The performance tests and chemical characterizations meet current Chinese national or international standards. In this study, the selected pipes and joints were static for a certain period of time. So, the performance of pipes and joints tends to stabilize after the accelerated aging test. Moreover, the test results are the average of the five sets of parallel measurements. In the five parallel experiments, each group of joints, both with and without aging specimens, originated from the same joint. The specific test scheme is outlined in Table 3. Shore hardness grades are adopted for the hardness test. Within each group, there are three test pieces of the same type, from which six test points are selected for each test piece, resulting in a total of 18 test values for the Shore hardness test results of this group of test pieces. Figure 2 illustrates the schematic diagram of hardness measurement points on the sample of PB and BFWJ. The accelerated aging test maintains consistency in this study by controlling aging time as a single variable. Additionally, mechanical property measurements and the preparation and handling of test samples adhere to relevant national or international standards.

When PB and BFWJ were tested by Attenuated Total Fourier Transform Reflection Infrared Spectroscopy (ATR FT-IR), the FTIR-650S, produced by Tianjin GangDong Scientific and Technology Co., Ltd., was employed to characterize the microstructure of the exposed surface of PB and BFWJ. The sample surface was kept clean before testing. A 400–6000  $\text{cm}^{-1}$  test band was selected, the scan rate was 32, and the resolution was adjusted to 4  $\text{cm}^{-1}$ .

The micro-morphological changes of the specimen's fracture surface during tensile failure were observed using the Helios5 CX scanning electron microscope from American Fei. The sample was cut into cubes with a side length of 1 cm. These cube samples were cleaned again, subjected to gold treatment, and left to stand for over 2 h before SEM examination.

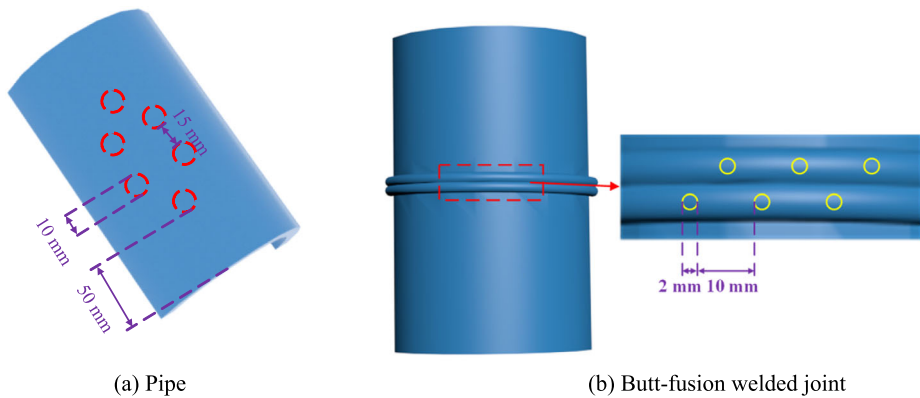


**Fig. 2** Schematic diagram of hardness measurement points on the sample

### 3 Results and discussion

#### 3.1 Impact properties

Figure 3 displays the impact strength of PB and BFWJ after undergoing various aging methods. The impact strength of both materials exhibits a decreasing trend with increasing AT after different aging methods of PB and BFWJ (Chen et al. 2023). The difference in impact strength between the two unaged materials was  $0.52 \text{ kJ/m}^2$ , and the decline curves were linear under thermal oxidative accelerated aging conditions. After 480 h, the impact strength of the pipe body began to decrease more rapidly, while the butt-fusion welded joint exhibited a slower rate of decline. By 960 h, the difference in impact strength between PB and BFWJ was only  $0.32 \text{ kJ/m}^2$ . The impact strength of the two materials tended to approach each other with increasing thermal-oxidative aging time.

Under hydrothermal aging conditions, the impact strength difference between PB and BFWJ remained stable before 240 h. The impact strength curve of the pipe body showed a noticeable concavity compared to the butt-fusion welded joint at 240–600 h, and the difference between PB and BFWJ decreased to  $0.43 \text{ kJ/m}^2$  at 960 h.

With an increase in AT, the molecular long chains of PB and BFWJ undergo breaking and cross-linking. Butt-fusion welded joint is a secondary processing product after high-temperature treatment. When the PB and BFWJ are not aged, their impact resistance differs. This is because some high polyethylene molecular chains (HPMC) are cross-linked and broken, and their spatial positions are altered. The trend of impact resistance in PB and BFWJ is inversely proportional to time.

#### 3.2 Tensile properties

Figure 4 illustrates that the tensile strength of PB and BFWJ is reduced as the AT increases. During thermal-oxidative aging, the tensile strength of the pipe body decreased by  $4.81 \text{ kJ/m}^2$ . Between 720 and 960 h, the tensile strength of the pipe dropped from  $21.77 \text{ kJ/m}^2$  to  $19.04 \text{ kJ/m}^2$ , accounting for a total reduction of 56.76%.

In thermal-oxidative aging and hydrothermal aging, the change in tensile strength for the butt-fusion welded joint and the pipe followed a similar pattern to the impact strength discussed in Sect. 3.1. At 960 h under thermal-oxidative aging conditions, the difference

**Fig. 3** The impact strength of PB and BFWJ after undergoing various aging methods

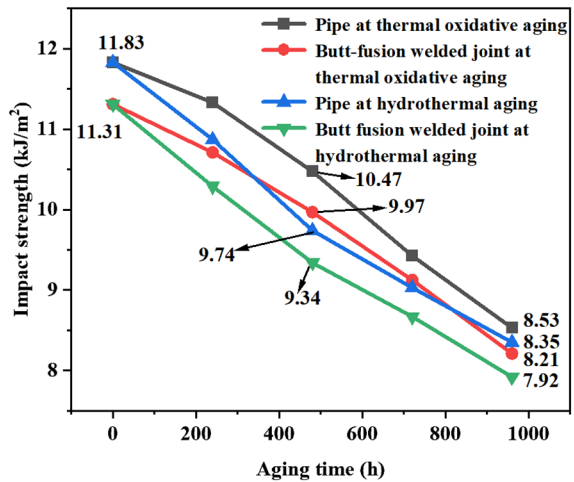
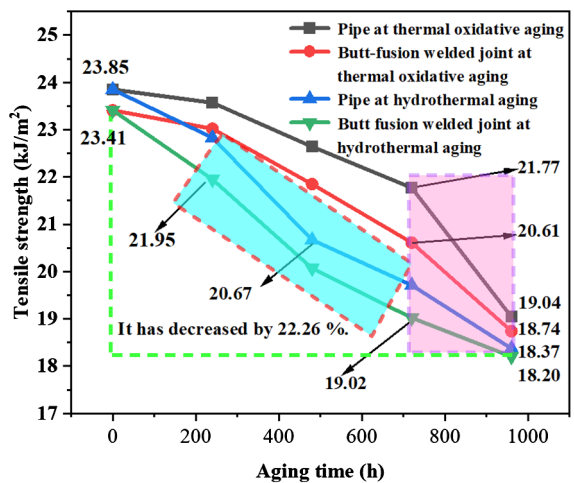


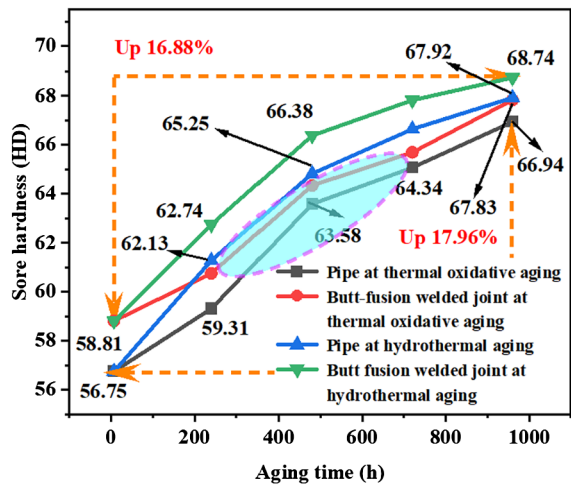
**Fig. 4** The tensile strength of PB and BFWJ after various aging methods



in tensile strength between PB and BFWJ decreased from  $0.44 \text{ kJ/m}^2$  to  $0.30 \text{ kJ/m}^2$ . The tensile strength of the pipe decreased by  $4.81 \text{ kJ/m}^2$ , while that of the butt-fusion welded joint decreased by  $4.67 \text{ kJ/m}^2$ . It represents  $22.98\%$  and  $22.26\%$  reductions for the pipe and butt-fusion welded joint, respectively. It indicates that the influence of aging on the tensile strength is greater for the pipe than for the butt-fusion welded joint.

The molecular chain of PB and BFWJ changes along with AT. Microscopically, the relative position of HPMC has altered, and weak molecular bonds have absorbed energy. On a macro level, the tensile strength of PB and BFWJ gradually decreases. It may be attributed to two factors. Firstly, aging reduces molecular spacing and increases cross-linking density (Ma et al. 2020). Secondly, molecular bonds absorb energy and break (Saba et al. 2016). The fluidity of the molecular chains at the interface of HDPE fiber increases, leading to a decrease in interfacial adhesion (Gong et al. 2021). A portion of the HPMC in the butt-fusion welded joint is broken and cross-linked due to high-temperature treatment during fabrication. As a result, the tensile strength of the butt-fusion welded joint is lower than that of the pipe. However, the molecules in the pipe body remain unchanged before aging, and more

**Fig. 5** The surface hardness of PB and BFWJ after undergoing different aging



molecules per unit volume in the pipe can undergo aging reactions compared to the butt-fusion welded joint. Consequently, the difference in tensile strength between PB and BFWJ is diminishing. As the AT increases, the pipe body is more prone to aging reactions than the butt-fusion welded joint. Therefore, the reduction in tensile strength of the pipe body during thermal-oxidative aging and hydrothermal aging is greater than that of the butt-fusion welded joint.

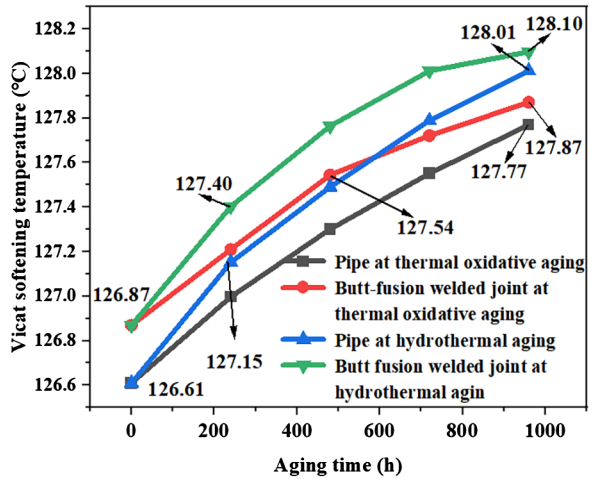
### 3.3 Hardness

Figure 5 illustrates the surface hardness of PB and BFWJ after undergoing different aging. The results indicate that both the surface hardness of PB and BFWJ has increased. Specifically, the surface hardness of the pipe body has increased by 17.96%, while the surface hardness of the butt-fusion welded joint has increased by 16.88% during hydrothermal aging. The hardness curve of the pipe body exhibits a “convex shape” between 240 h and 720 h after undergoing various accelerated aging methods. As AT progresses from 240 h to 480 h, the molecular chain of the pipe body undergoes cross-linking and chain breaking. It leads to a reduction in the relative distance between molecular chains and an increase in the relative distance between macromolecular groups. Consequently, the pathways for water and oxygen molecules to participate in chemical reactions within molecular groups are expanded, resulting in an increased diffusion rate of water and oxygen molecules.

### 3.4 Vicat softening temperature

Figure 6 displays the Vicat softening temperature of PB and BFWJ after undergoing various aging methods. Its Vicat softening temperature increases with the rise in AT. The Vicat softening temperature lines of PB and BFWJ exhibit an upward convex trend. The increase in Vicat softening temperature is pronounced in the pipe body compared to the butt-fusion welded joint. From a statistical perspective, the Vicat softening temperature of PB and BFWJ increased by 1.16 °C and 1.00 °C after 960 h of thermal-oxidative aging. During hydrothermal aging, the Vicat softening temperature of PB and BFWJ increased by 1.40 °C and 1.23 °C after 960 h. The period from 0 to 240 h represents the highest growth rate of the Vicat softening temperature of PB and BFWJ after undergoing various aging methods. The AT of

**Fig. 6** The Vicat softening temperature of PB and BFWJ after undergoing various aging methods



480 h serves as a turning point for the growth rate of the Vicat softening temperature of the material, with the growth rate being higher before 480 h than after.

### 3.5 Oxidation induction time

The OIT test can determine the antioxidant content of the specimen during an AT, indirectly reflecting the antioxidant activity of the sample. Figure 7 displays the OIT of PB and BFWJ after undergoing various aging methods. The gradual consumption of antioxidants is evident in the trend of PB and BFWJ during the two accelerated aging tests, indicating a gradual decline in the sample's oxidative resistance. Specifically, the OIT of PB and BFWJ is reduced by 27.80% and 30.37%, respectively, under thermal-oxidative aging conditions. After 960 h of hydrothermal aging, differential scanning calorimetry tests revealed similar reductions of 27.80% and 30.37%, respectively. The turning point of the OIT slope for the sample occurs at 480 h. Before this, the slope of the OIT for the pipe body was lower than that of the butt-fusion welded joint, whereas, after 480 h, it was the opposite. Consequently, the pipe body exhibits stronger anti-oxidation properties compared to the joint.

### 3.6 Attenuated total reflectance Fourier transform infrared spectroscopy

Figure 8 displays the infrared spectra of the pipe and butt-fusion welded joint after undergoing different aging methods for 960 h. The four curves exhibit similar absorption peaks, differing in absorbance intensity. These variations can be attributed to the aging of the PE, leading to changes in the disappearance and formation of internal functional groups. There are absorption peaks on both sides of  $2910\text{ cm}^{-1}$ , one at  $1460\text{ cm}^{-1}$  and another near  $720\text{ cm}^{-1}$ ; these are characteristic peaks of HDPE in the infrared spectrum. The absorption peaks on both sides of  $2910\text{ cm}^{-1}$  can be attributed to the symmetric and asymmetric stretching motions of CH. Similarly, the absorption peaks on both sides of  $1460\text{ cm}^{-1}$  are formed due to the bending action of CH. Additionally, the swing motion and deformation of long-molecular chains, consisting of at least four  $\text{CH}_2$ , have generated an absorption peak near  $720\text{ cm}^{-1}$ .

During thermal-oxidative aging or hydrothermal aging, the molecular chain of PB and BFWJ primarily undergoes cross-linking, chain breaking, and oxidation reactions. The ox-

**Fig. 7** The OIT of PB and BFWJ after undergoing various aging methods

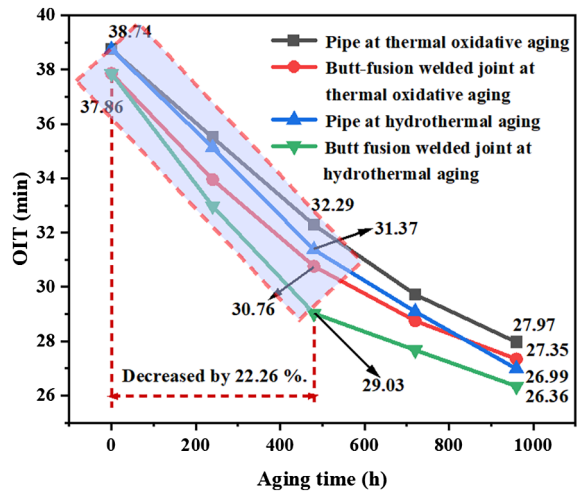


**Table 4** Absorption peaks corresponding to different functional groups

Functional groups	Wave number ( $\text{cm}^{-1}$ )
–OH, $\text{RC}\equiv\text{CR}$	3100–3700
$\text{RCHO}$ , $\text{RC}=\text{O}$ , $\text{RC}=\text{CR}$ , $\text{RCOOH}$	1530–1730
$\text{RC}-\text{O}-\text{CR}$ , $\text{RC}-\text{OH}$	950–1200

ation of HDPE produces oxidation products, most of which are molecular chains containing carbonyl and hydroxyl groups (Chen et al. 2023).

Table 4 presents absorption peaks corresponding to different functional groups. As examples, aldehyde, ester, and ketone groups ( $1710\text{--}1730\text{ cm}^{-1}$ ), carboxylic acid groups ( $1700\text{ cm}^{-1}$ ), structures containing OH groups ( $3100\text{--}3700\text{ cm}^{-1}$ ,  $1530\text{--}1640\text{ cm}^{-1}$ ), and C–O–C groups ( $1130\text{--}1210\text{ cm}^{-1}$ ) are considered indicators of aging in PE. These groups are collectively called functional groups associated with aging (Gong et al. 2021; Gedde and Ifwarson 1990). Upon examining the three regions in Fig. 8a, b, and c, it becomes evident that, for the bands between  $3100\text{--}3700\text{ cm}^{-1}$ ,  $1530\text{--}1730\text{ cm}^{-1}$ , and  $950\text{--}1200\text{ cm}^{-1}$ , the absorbance intensity of the pipe body is either lower or equal to that of the butt-fusion welded joint, during both thermal-oxidative aging and hydrothermal aging. It indicates that the content of OH, C=O, and C–O–C groups in the pipe body is lower than that in the butt-fusion welded joint.

During hydrothermal aging, at  $1730\text{ cm}^{-1}$ , the tensile vibration strength of the C=O group in the pipe body is greater than that in the butt-fusion welded joint. Similarly, at  $1640\text{ cm}^{-1}$  during hydrothermal aging, the tensile vibration strength of the C=C group in the pipe body is higher than in the butt-fusion welded joint. During hydrothermal aging, the pipe body exhibits higher tensile vibration strength of the C–O group at  $1050\text{ cm}^{-1}$  compared to the butt-fusion welded joint. These results suggest that the type of sample, specifically the butt-fusion welded joint, plays a significant role in the aging process, and the oxidation degree of the pipe body consistently remains lower than that of the butt-fusion welded joint during both thermal-oxidative aging and hydrothermal aging. This finding implies that the pipe body exhibits superior oxidation resistance, possibly due to variations in material composition or structural integrity. The FTIR data indicates that the overall trend

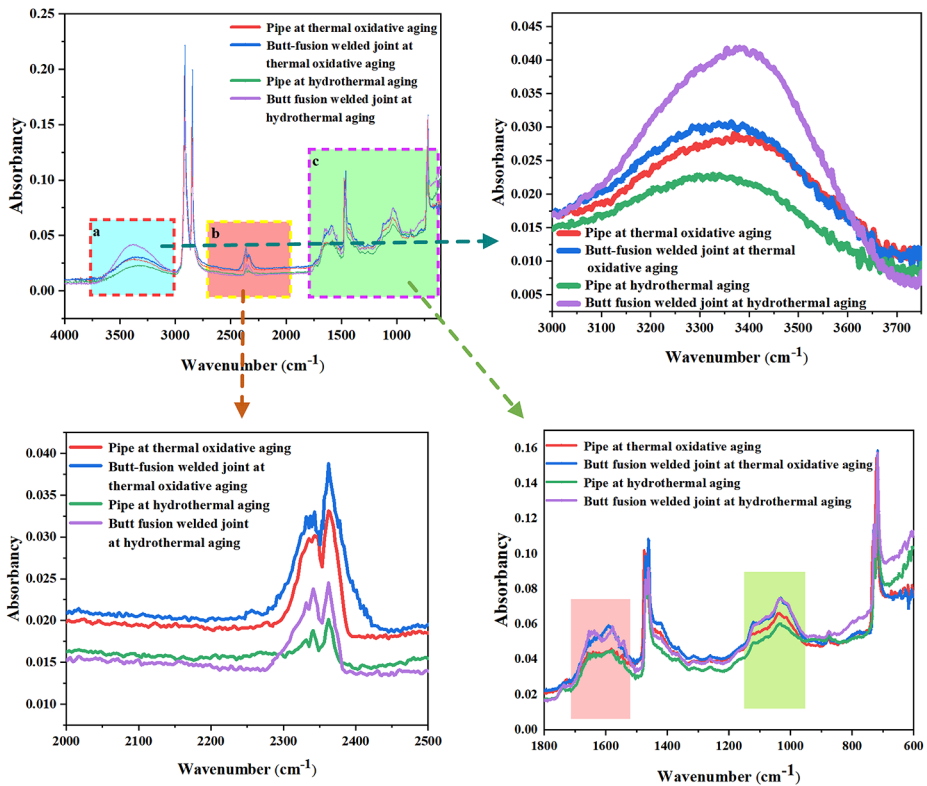


**Fig. 8** The infrared spectra of PB and BFWJ after undergoing different aging methods at 960 h

of the samples remains consistent, regardless of whether they undergo thermal-oxidative aging or hydrothermal aging. It implies that the carbon skeleton of the PB and BFWJ remains unchanged under both aging conditions.

### 3.7 Scanning electron microscope

Figure 9 displays the micro-surface morphology of fracture surfaces of PB and BFWJ under thermal-oxidative aging at various time intervals. At 960 h of thermal-oxidative aging, undulations and depressions are observed on the fractures of PB and BFWJ. Additionally, the number of small fibers at the end of the fiber is lower in the aging samples of the pipe body compared to those in the butt-fusion welded joint during thermal-oxidative aging. Furthermore, the degree of depression at the fracture of the pipe body is significantly lower than in the butt-fusion welded joint.

The disparity in fiber characteristics between PB and BFWJ arises because the butt-fusion welded joint undergoes secondary processing. The high-temperature treatment experienced by the pipe body at the interface during processing leads to the cross-linking of certain molecular chains, oxidation of others, and the breaking or rupture of molecular bonds within the chains due to energy absorption. Consequently, distinct variations in the micromorphology of the fracture surface between PB and BFWJ are observed. In Fig. 9, panels a and b show that the number of fibers in the pipe body is lower than in the butt-fusion welded

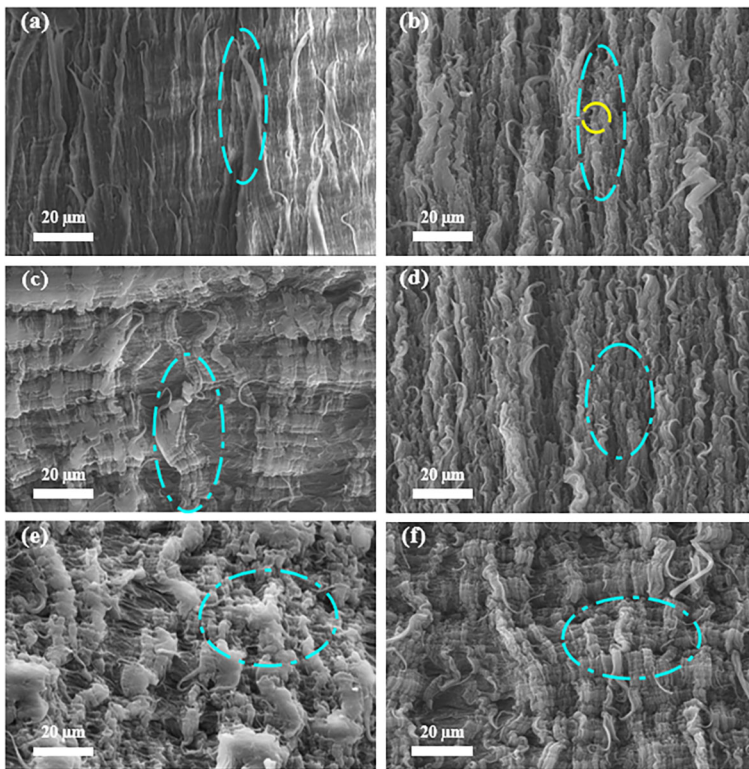


**Fig. 9** Micro-surface morphology of fracture surfaces of PB and BFWJ under thermal-oxidative aging at different times: (a) pipe not aged, (b) butt-fusion welded joint not aged, (c) pipe at 480 h, (d) butt-fusion welded joint at 480 h, (e) pipe at 960 h, and (f) butt-fusion welded joint at 960 h

joint, and the roughness of the fracture surface in the pipe body is comparatively reduced, especially in the unaged samples.

Figure 10 illustrates the micro-surface morphology of fracture surfaces of PB and BFWJ under hydrothermal aging at different time intervals. At the same AT, the maximum diameter of the concave part of the pipe body during hydrothermal aging is smaller than in the butt-fusion welded joint. For instance, in Figures c and d of Fig. 10, it is evident that the maximum diameter of the concave part of the pipe body ( $29.33\ \mu\text{m}$ ) is  $9.33\ \mu\text{m}$  shorter than that of the butt-fusion welded joint ( $38.66\ \mu\text{m}$ ) during hydrothermal aging. Moreover, as AT increases, the surface undulation of the PB and BFWJ fracture becomes progressively more apparent.

The molecular chains in the pipe body undergo an oxidation reaction, resulting in cross-linking and chain-breaking. As the aging temperature (AT) increases, the intensity of the oxidation reaction grows, leading to enhanced mobility of molecular chains at the interface of HDPE fibers. This increased mobility reduces interfacial adhesion (Vijayan et al. 2016; Yan et al. 2019). The microstructure of the fracture surface displays a greater degree of concavity and convexity, along with a higher quantity of fibers, in the case of the pipe body. Some molecular chains in the butt-fusion welded joint undergo alterations during production. Additionally, in its unaged state, the butt-fusion welded joint exhibits a higher degree of aging compared to the pipe body.

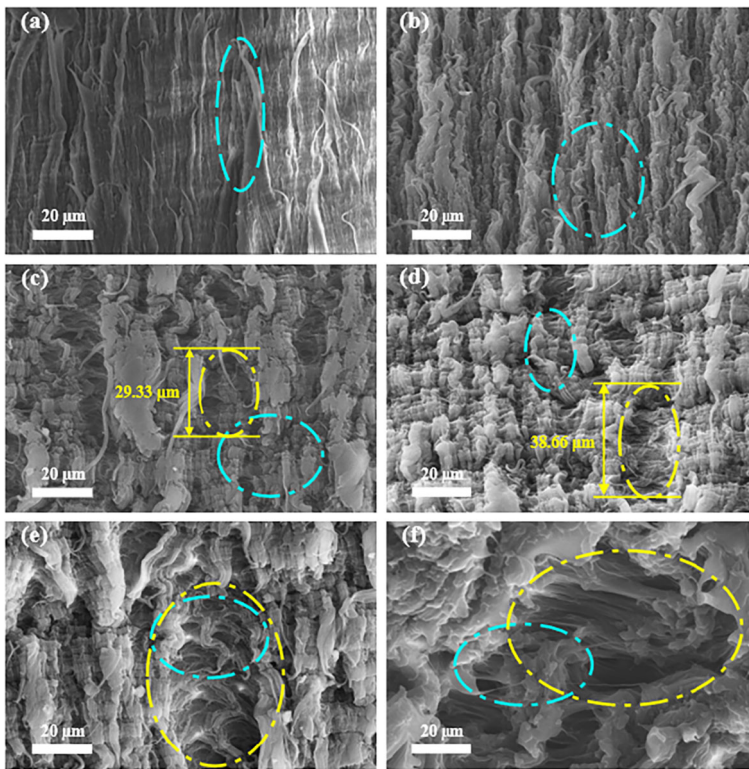


**Fig. 10** Micro-surface morphology of fracture surfaces of PB and BFWJ under hydrothermal aging at different times: (a) pipe not aged, (b) butt-fusion welded joint not aged, (c) pipe at 480 h, (d) butt-fusion welded joint at 480 h, (e) pipe at 960 h, and (f) butt-fusion welded joint at 960 h

As the AT increases, the oxidation reaction in the butt-fusion welded joint intensifies, resulting in greater damage to the interface between fibers. It leads to decreased intermolecular interactions and a lower adhesive strength between the fibers compared to the initial state (Wu et al. 2021; Sun et al. 2022). The degree of concavity and convexity increases in the microstructure of the fracture surface. It is accompanied by an increased quantity of fibers for the butt-fusion welded joint. When viewed from a microscopic perspective with the same aging time, the surface roughness and fiber quantity of the pipe body are lower than those of the butt-fusion welded joint. Additionally, this difference tends to decrease with increasing AT. There is a considerable influence of H<sub>2</sub>O in the aging of PB and BFWJ, intensifying the aging reaction of the material and extending the aging reaction towards the interior of the material.

Due to oxidation and hydrolysis degradation, the cross-linking and fracture among polyethylene molecules intensify. It leads to the expansion and deepening of the damaged area at the interface between fibers in polyethylene. Consequently, intermolecular interaction decreases, and the bonding strength between fibers decreases significantly (Wu et al. 2021; Yang et al. 2015). A “pit” becomes evident at the fracture section of the specimen. It is due to alterations in the molecular chains of the butt-fusion welded joint during processing and manufacturing. When exposed to hydrothermal accelerated aging under identical conditions, the degree of aging in the pipe body is lower than that in the butt-fusion welded joint.

It is manifested microscopically by a smaller maximum surface diameter of the pipe fracture compared to the butt-fusion welded joint. Under different aging methods, the microscopic characteristics represented by SEM of PB and BFWJ are consistent with the mechanical properties of PB and BFWJ in Sects. 3.1 and 3.2.

## 4 Ageing mechanisms discussion

Based on the above results, the regular aging trend and degree of PB and BFWJ can be summarized. On the one hand, as the AT increases, the impact strength, tensile strength, and OIT of PB and BFWJ significantly decrease. In contrast, the hardness, Vicat softening temperature, and concentration of aging radicals gradually increase. On the other hand, there are initial differences in various mechanical properties between PB and BFWJ before accelerated aging. These differences exhibit a decreasing trend with extended AT exposure. It is related to the concentration of groups in the material that have not undergone aging reactions. After 960 h of accelerated aging under two distinct aging conditions, the aging degree of PB and BFWJ did not reach a level similar to the actual working conditions. In actual engineering, observable aging phenomena occur in high-density polyethylene pipelines used for long-term operation (Wu et al. 2021). Figures 9(a) and 10(a) in Sect. 3.7 reveal variations in the length and density of broken fibers when PB and BFWJ were not subjected to aging. Additionally, Fig. 8(a) in Sect. 3.6 shows slight peaks, such as those around  $950\text{--}1200\text{ cm}^{-1}$ ,  $1530\text{--}1730\text{ cm}^{-1}$ , and  $3100\text{--}3700\text{ cm}^{-1}$ , indicative of polyethylene aging.

Figure 11 illustrates the aging mechanism diagram of PB and BFWJ subjected to thermal-oxidative aging. Macroscopically, these changes are evident in heightened material brittleness, reduced impact strength and tensile strength, and amplified hardness. On a microscopic level, there is an augmentation in the presence of age groups within the material. This process entails infiltrating oxygen molecules into the interior of PB and BFWJ. Subsequently, aging reactions occur between  $\text{O}_2$  and polyethylene molecules, forming new molecular groups that are both larger and more intricate compared to the unaltered polyethylene molecules. As the AT rises, the degree of cross-linking in polyethylene advances, resulting in an augmentation of cross-linked polyethylene molecular groups and an increase in the number of age groups like aldehyde and carboxyl groups. Furthermore, a significant increase in the quantity of fibers was observed on the fractured material surface. It is essential to acknowledge that inherent disparities in mechanical and chemical properties exist between the pipe body and the butt-fusion welded joint, even before aging. These differences arise from alterations in the internal molecular structure, spatial positioning, and molecular chain end groups that transpire during the production process of the butt-fusion welded joint. Specifically, during the high-temperature joining process, wherein both ends of the pipe are connected, some polyethylene molecules in the heat-affected zone undergo cross-linking and aging reactions with oxygen and water molecules in the atmosphere, forming age groups. Prior to aging, the mechanical properties of the pipe body surpass those of the butt-fusion welded joint. An SEM examination reveals a significantly lower quantity of fibers on the fractured surface of the pipe body in contrast to the butt-fusion welded joint.

Figure 12 displays the aging mechanism diagram of PB and BFWJ under hydrothermal aging conditions. In this environment, water and oxygen molecules penetrate the interior of the test specimen, initiating aging reactions with polyethylene molecules. It leads to the formation of aging groups containing aldehyde and carboxyl groups. The effects of hydrothermal aging are comparable to those of thermal-oxidative aging, resulting in an increase in the degree of cross-linking, a greater number of cross-linked polyethylene molecular groups,

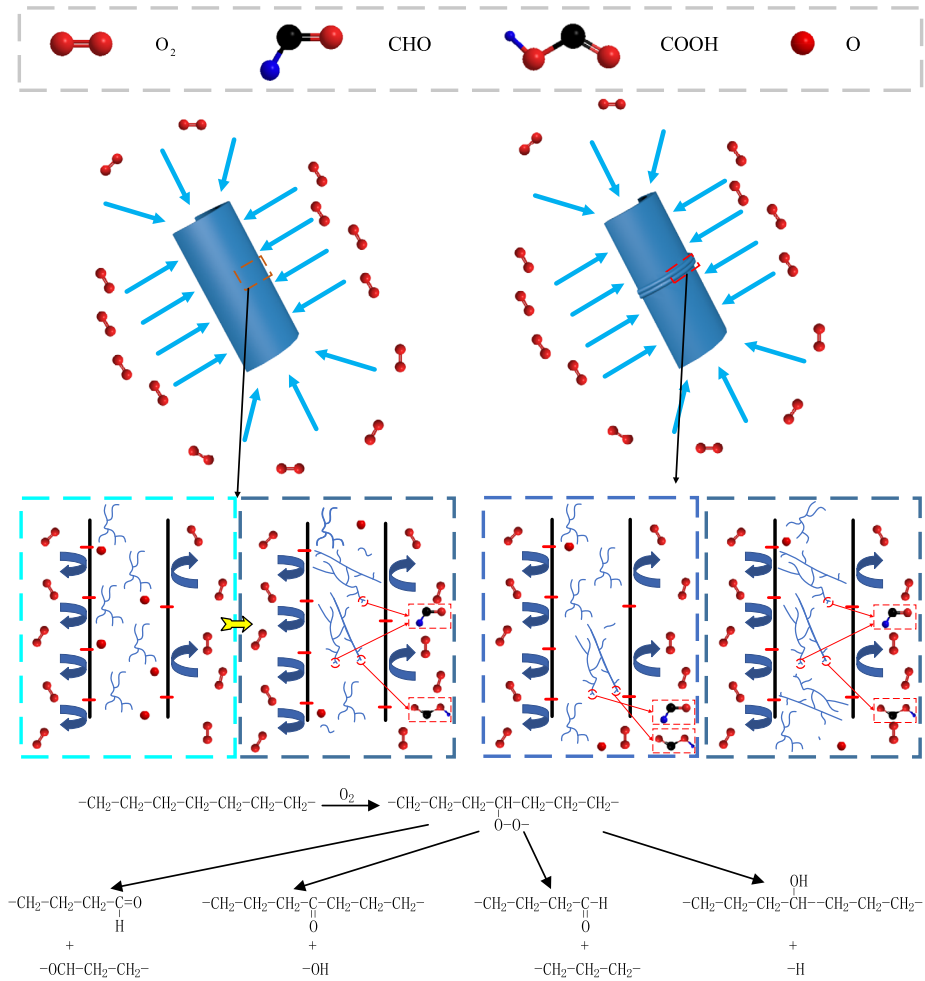


**Fig. 11** The aging mechanism diagram of PB and BFWJ under thermal-oxidative aging

and an augmentation in aging groups like aldehyde and carboxyl groups. Notably, the degree of cross-linking surpasses that observed in thermal-oxidative aging. During hydrothermal aging, at the microscopic level, a more intricate network structure forms through the cross-linking of polyethylene molecules compared to thermal-oxidative aging. This heightened complexity arises from the increased involvement of water molecules in the aging reaction of polyethylene, leading to a higher count of hydroxyl groups. Consequently, the quantity of hydroxyl groups produced during hydrothermal aging exceeds that of thermal-oxidative aging. Macro performance results closely mirror those in specimens subjected to thermal oxygen aging. SEM reveals that the depression range on the fracture surface of the pipe body is significantly lower than that of the butt-fusion welded joint.

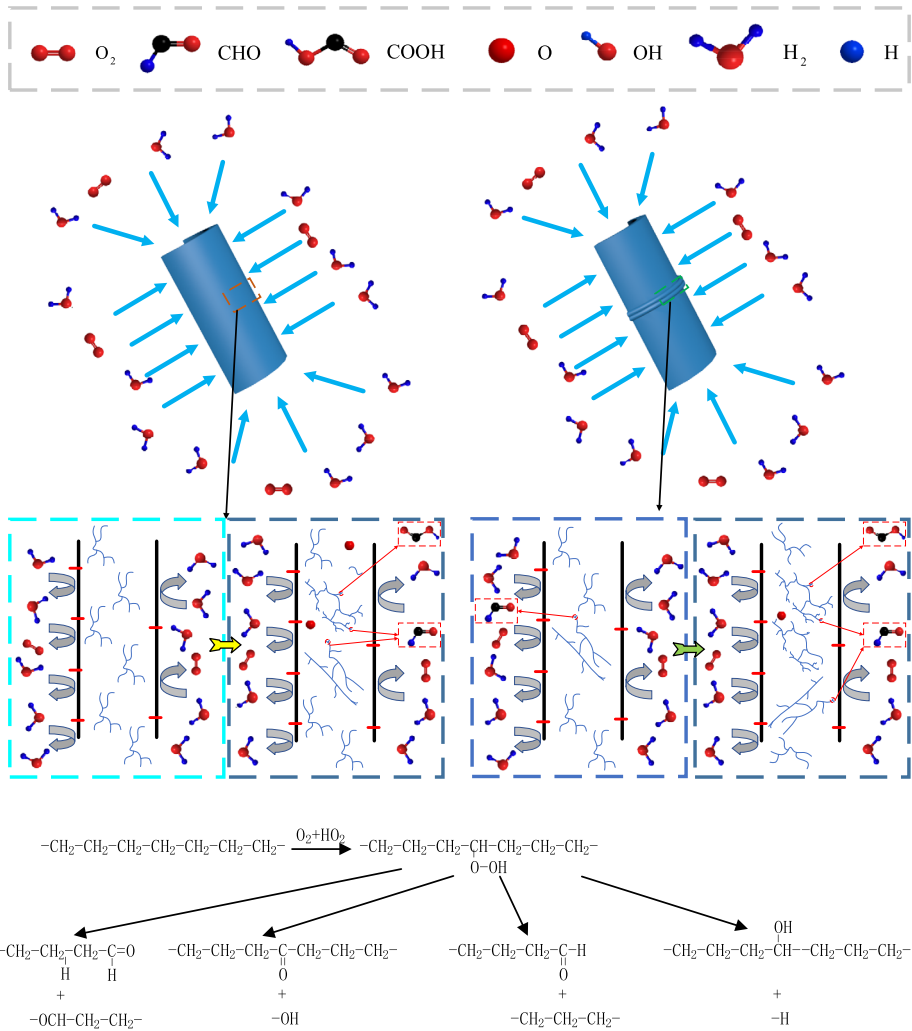


Fig. 12 The aging mechanism diagram of PB and BFWJ under hydrothermal aging

## 5 Conclusions

In this study, thermal-oxidative accelerated aging and hydrothermal accelerated aging methods were employed to evaluate the mechanical and chemical properties of the pipe body and butt-fusion welded joint. Initially, the performance matrices, such as tensile strength and impact strength for the pipe body and the butt-fusion welded joint, surpass those of the latter. However, the hardness and Vicat softening temperature of the pipe body are relatively lower compared to those of the butt-fusion welded joint. The OIT of the pipe body closely aligns with that of the butt-fusion welded joint. The initial discrepancies in mechanical properties between the pipe body and butt-fusion welded joint exhibit a decreasing trend with increasing AT. In the spectral bands of  $3100\text{--}3700\text{ cm}^{-1}$ ,  $1530\text{--}1730\text{ cm}^{-1}$ ,  $950\text{--}1200\text{ cm}^{-1}$ , and  $700\text{--}780\text{ cm}^{-1}$ , the absorbance intensity of the pipe body is either less than or equal to that

of the butt-fusion welded joint. The number of functional groups like aldehydes, esters, ketones, and carboxylic acids in the pipe body is lower than that in the butt-fusion welded joint. The number of aging byproducts, such as aldehydes and carboxylic acids, produced during the aging process of the polyethylene pipe is lesser compared to that of the butt-fusion welded joint.

**Acknowledgements** The State Administration provided exceptional technical support for Market Regulation (2021YJ021).

Patent transformation project in autonomous region by Market Supervision Administration of Xinjiang Uygur Autonomous Region (20230030).

This work was supported in part by the science and technology plan project of the general administration of market supervision (2021MK118)

Regional collaborative innovation project of the autonomous region (science and technology aid plan for Xinjiang) (2021E02050).

**Author contributions** Y.C.C made the conceptualization, provided methodology and acquired the financial support for the project leading to this publication. J.Y wrote the main manuscript text, prepared figures, analysed data, conducted a research and investigation process. Y.F.L analysed data, provided study materials, the support of software, supervision, project administration. R.M provided study materials and supervision. Q.L project administration and supervision. X.L.F provided study materials and project administration. All authors reviewed the manuscript.

**Data Availability** No datasets were generated or analysed during the current study.

## Declarations

**Competing interests** The authors declare no competing interests.

## References

- Badia, J.D., Santonja-Blasco, L., Martínez-Felipe, A., et al.: Hygrothermal ageing of reprocessed polylactide. *Polym. Degrad. Stab.* **97**(10), 1881–1890 (2012)
- Barker, M.B., Bowman, J., Bevis, M.: The performance and causes of failure of polyethylene pipes subjected to constant and fluctuating internal pressure loadings. *J. Mater. Sci.* **18**, 1095–1118 (1983)
- Bhowmick, A.K., White, J.R.: Thermal, UV- and sunlight ageing of thermoplastic elastomeric natural rubber-polyethylene blends. *J. Mater. Sci.* **37**(23), 5141–5151 (2002)
- Blivet, C., Larché, J.F., Israëli, Y., et al.: Thermal oxidation of cross-linked PE and EPR used as insulation materials: multi-scale correlation over a wide range of temperatures. *Polym. Test.* **93**, 106913 (2021)
- Bracco, P., Costa, L., Luda, M.P., et al.: A review of experimental studies of the role of free-radicals in polyethylene oxidation. *Polym. Degrad. Stab.* **155**, 67–83 (2018)
- Chaoui, K., Khelif, R., Zeghib, N., et al.: Failure Analysis of Polyethylene Gas Pipes. Safety, Reliability and Risks Associated with Water, Oil and Gas Pipelines, pp. 131–163. Springer, Netherlands (2008)
- Chen, H., Scavuzzo, R.J., Srivatsan, T.S.: Influence of joining on the fatigue and fracture behavior of high density polyethylene pipe. *J. Mater. Eng. Perform.* **6**, 473–480 (1997)
- Chen, G., Yang, Y., Zhou, C., et al.: Thermal-oxidative aging performance and life prediction of polyethylene pipe under cyclic and constant internal pressure. *J. Appl. Polym. Sci.* (2019)
- Chen, Y.C., Li, Y.F., Xi, Y., et al.: Natural aging mechanism of buried polyethylene pipelines during long-term service. *Pet. Sci.* (2023)
- Choi, B.-Ho., et al.: Fracture initiation associated with chemical degradation: observation and modeling. *Int. J. Solids Struct.* **681**–695 (2005)
- Erdmann, M., Böhning, M., Niebergall, U.: Physical and chemical effects of biodiesel storage on high-density polyethylene: evidence of co-oxidation. *Polym. Degrad. Stab.* **161**, 139–149 (2019)
- Esaklul, K.A., Jim, M.: Nonmetallics applications in oil and gas production (pipes, liners, rehabilitations). *Trends in Oil and Gas Corrosion Research and Technologies* 627–660 (2017)
- Frederick, C., Allen, P., David, Z.: High-density polyethylene piping butt-fusion joint examination using ultrasonic phased array (2010)

- GB/T 19810—2005 Polyethylene (PE) pipes and fittings - Determination of tensile strength and failure mode of butt-fusion joints (2005)
- GB/T 38119-2019 Verification of Shore durometers (2019)
- GB/T 1043.1-2008 Plastics—Determination of Charpy impact properties—Part 1: Non-instrumented impact test (2008)
- GB/T 19466.6-2009 Plastics—Differential scanning calorimetry (DSC)—Part 6: Determination of oxidation induction time (isothermal OIT) and oxidation induction temperature (dynamic OIT) (2009)
- Gedde, U.W., Ifwarson, M.: Molecular structure and morphology of crosslinked polyethylene in an aged hot-water pipe. *Polym. Eng. Sci.* **30**(4), 202–210 (1990)
- Ghabeche, W., Chaoui, K., Zeghib, N.: Mechanical properties and surface roughness assessment of outer and inner HDPE pipe layers after exposure to toluene methanol mixture. *Int. J. Adv. Manuf. Technol.* **103**, 2207–2225 (2019)
- Gong, Y., Wang, S.H., Zhang, Z.Y., et al.: Degradation of sunlight exposure on the high-density polyethylene (HDPE) pipes for transportation of natural gases. *Polym. Degrad. Stab.* **194**, 109752 (2021)
- Hoàng, E.M., Lowe, D.: Lifetime prediction of a blue PE100 water pipe. *Polym. Degrad. Stab.* (2008)
- ISO 179-1-2010 Plastics—Determination of Charpy impact properties—Part 1: Non-instrumented impact test (2010)
- ISO 13953—2001 Polyethylene (PE) pipes and fittings - Determination of tensile strength and failure mode of butt-fusion joints (2001)
- ISO 2507-1-1995 Thermoplastics pipes and fittings—Vicat softening temperature—Part 1: General test method (1995)
- ISO 11357-6-2013 Plastics. Differential scanning calorimetry (DSC). Part 6: Determination of oxidation induction time (isothermal OIT) and oxidation induction temperature (dynamic OIT) (2013)
- Kato, M., Osawa, Z.: Effect of stereoregularity on the thermo-oxidative degradation of polypropylenes. *Polym. Degrad. Stab.* **65**(3), 457–461 (1999)
- Konica, S., Sain, T.: A thermodynamically consistent chemo-mechanically coupled large deformation model for polymer oxidation. *J. Mech. Phys. Solids* **137**, 103858 (2020)
- Lai, H., Fan, D., Liu, K.: The effect of welding defects on the long-term performance of HDPE pipes. *Polymers* **14**(19), 3936 (2022)
- Leskovics, K., Kollár, M., Bárczy, P.: A study of structure and mechanical properties of welded joints in polyethylene pipes. *Mater. Sci. Eng.* (2006)
- Ma, S., He, Y., Hui, L., et al.: Effects of hygrothermal and thermal aging on the low-velocity impact properties of carbon fiber composites. *Adv. Compos. Mater.* **29**(1), 55–72 (2020)
- Murch, M.G., Troughton, M.J.: a study of the applicability of the tensile weld test for thick walled polyethylene pipe. *TWI Journal* (1998)
- Oluwoye, I., Altarawneh, M., Gore, J., et al.: Oxidation of crystalline polyethylene. *Combust. Flame* **162**(10), 3681–3690 (2015)
- Oluwoye, I., Altarawneh, M., Gore, J., et al.: Oxidation of polyethylene under corrosive NO<sub>x</sub> atmosphere. *J. Phys. Chem. C* **120**(7), 3766–3775 (2016)
- Pinter, G., Lang, R.W.: Effect of stabilization on creep crack growth in high-density polyethylene. *J. Appl. Polym. Sci.* **90**(12), 3191–3207 (2003)
- Pospišil, J., Horák, Z., Pilař, J., et al.: Influence of testing conditions on the performance and durability of polymer stabilisers in thermal oxidation. *Polym. Degrad. Stab.* **82**(2), 145–162 (2003)
- Saba, N., Jawaid, M., Alotman, O.Y., et al.: A review on dynamic mechanical properties of natural fibre reinforced polymer composites. *Constr. Build. Mater.* **106**, 149–159 (2016)
- Sun, Y., et al.: Effects of stitch yarns on interlaminar shear behavior of three-dimensional stitched carbon fiber epoxy composites at room temperature and high temperature. *Advanced Composites and Hybrid Materials* (2022)
- Taheri, F.: *Advanced Fiber-Reinforced Polymer (FRP) Composites for the Manufacture and Rehabilitation of Pipes and Tanks in the Oil and Gas Industry*. Advanced Fibre-Reinforced Polymer (FRP) Composites for Structural Applications. Woodhead Publishing (2013)
- Vijayan, V., Pokharel, P., Kang, M.K., et al.: Thermal and mechanical properties of e-beam irradiated butt-fusion joint in high-density polyethylene pipes. *Radiat. Phys. Chem.* **122**, 108–116 (2016)
- Wang, Q., Zhou, H., Xie, J., et al.: Nonlinear ultrasonic evaluation of high-density polyethylene natural gas pipe butt-fusion welded joint aging behavior. *Int. J. Press. Vessels Piping* **189**, 104272 (2021)
- Whelton, A.J., Dietrich, A.M.: Critical considerations for the accelerated aging of high-density polyethylene potable water materials. *Polym. Degrad. Stab.* (2009)
- Wu, Y., Xun, L., Huang, S., et al.: Crack spatial distributions and dynamic thermomechanical properties of 3D braided composites during thermal oxygen ageing. *Composites, Part A, Appl. Sci. Manuf.* **144**, 106355 (2021)

- Yan, D., Zhang, H., Lu, S., et al.: Synergistic modification effect of polyvinylidene fluoride and polydopamine on mechanical and damping properties of three-dimensional braided carbon fibers reinforced composites. *J. Mater. Sci.* **54**(7), 5457–5471 (2019)
- Yang, B., Zhang, J., Zhou, L., et al.: Effect of fiber surface modification on water absorption and hydrothermal aging behaviors of GF/pCBT composites. *Composites, Part B, Eng.* **82**, 84–91 (2015)
- Zheng, J., Zhong, S., Shi, J., et al.: Study on the allowable temperature for preventing over welding during thermal welding of polyethylene pipe. *J. Press. Vessel Technol.* **137**(2), 021401 (2015)

**Publisher's Note** Springer Nature remains neutral with regard to jurisdictional claims in published maps and institutional affiliations.

Springer Nature or its licensor (e.g. a society or other partner) holds exclusive rights to this article under a publishing agreement with the author(s) or other rightsholder(s); author self-archiving of the accepted manuscript version of this article is solely governed by the terms of such publishing agreement and applicable law.